Traffic 2003; **4:** 460–467
Blackwell Munksgaard

ISSN 1398-9219

Movement of Plasma-Membrane-Associated Clathrin Spots Along the Microtubule Cytoskeleton

Joshua Z. Rappoport[1], Bushra W. Taha[1] and Sanford M. Simon[1,*]

[1]The Laboratory of Cellular Biophysics, The Rockefeller University, 1230 York Avenue, Box 304, New York, New York, 10021, USA
** Corresponding author: Sanford M. Simon, simon@rockefeller.edu*

The current understanding of the role of plasma-membrane-associated clathrin suggests that clathrin-coated pits form at the sites of activated receptors and then, following internalization, the clathrin coat is rapidly shed. Utilizing total internal reflection fluorescence microscopy (TIR-FM), we have documented linear lateral motion of cell-surface-associated dsRed-clathrin spots parallel to the plasma membrane. Clathrin spot motility was observed in multiple cell lines (MDCK, CHO, Cos-7 and HeLa). In MDCK cells dsRed-clathrin spots moved along linear pathways up to 4 μm in length with rates of approximately 0.8 μm/s. Spots did not generally undergo internalization during movement. The motion of these puncta was coincident with the microtubule cytoskeleton, and depolymerization of microtubules reduced spot motility over 10-fold. Over-expression of the microtubule-associated protein tau-EGFP decreased spot run length by 40% without affecting the rate of movement. Thus dsRed-clathrin puncta move along the microtubule cytoskeleton parallel to the cell surface.

Key words: clathrin, evanescent wave microscopy, microtubules, tau, total internal reflection fluorescence microscopy (TIR-FM)

Received 31 January 2003, revised and accepted for publication 31 March 2003

The production of clathrin-coated vesicles occurs at both the *trans*-Golgi and the plasma membrane and is important in the anterograde transport of biosynthetic cargo and the endocytosis of molecules from the cell surface, respectively (1–3). Although a great deal is known regarding the process of receptor-mediated endocytosis, the precise biophysical role of the clathrin coat and the exact function of each of the multiple adapter and accessory proteins involved in the production and fission of coated vesicles remains to be fully elucidated (2–6). Recent advances in live cell imaging permit real-time analysis of membrane trafficking. The technique of total internal reflection fluorescence microscopy (TIR-FM) has permitted a highly sensitive examination of the events occurring within ~100 nm of the plasma membrane (7,8). Studies performed by our laboratory and others have utilized TIR-FM to image processes such as exocytosis, cell adhesion, cytoskeletal organization, and more recently endocytosis (7–11)s.

Although much focus has been directed at the study of actin in endocytosis (10,12,13), some observations suggest a possible role for the microtubule cytoskeleton (14–16). While it has previously been observed that drugs that depolymerize microtubules can down-regulate endocytosis (14,16), these studies generally concluded that these effects were due to a bottleneck in microtubule-based endocytic vesicle transport subsequent to the shedding of the clathrin coat (12,16). Additionally, the inability to demonstrate an association between clathrin and tubulin *in vitro* has led many to conclude that a biologically relevant interaction between clathrin-coated vesicles and microtubules does not exist (17,18). However, the recent observation that part of the adaptin complex involved in post-Golgi clathrin coat formation can, in fact, bind to microtubules raises the issue of whether there may exist a similar interaction between plasma membrane-associated clathrin coat components and the microtubule cytoskeleton (18).

The current understanding of the biophysical role of plasma membrane clathrin does not predict motion of clathrin-coated structures parallel to the plane of the cell surface. In the case of endocytosis it is believed that clathrin triskelions polymerize at the sites of activated receptors and, subsequent to pit formation and fission, the clathrin coat is rapidly shed (2,12,19). The suggestion that the formation and dissolution of clathrin coats occur at the sites of endocytosis immediately prior to and following internalization, respectively, implies that the functional role of the clathrin coat does not go beyond the budding process.

TIR-FM has permitted us to evaluate the behavior of plasma-membrane-associated clathrin puncta. In studies previously performed in migrating MDCK cells clathrin puncta, bound to dynamin2, were observed to exist for extended periods on the plasma membrane prior to endocytosis (20). A subset of clathrin spots was observed to move laterally, parallel to the membrane surface. In this study we report the lateral movement of clathrin puncta in multiple cell lines (MDCK, CHO, Cos-7 and HeLa). These dsRed-clathrin puncta moved along the microtubule

cytoskeleton. Further, the lateral motility of clathrin spots was sensitive to disruption of microtubules by nocodazole treatment. Over-expression of the microtubule-associated protein tau decreased the run length of the clathrin puncta, but not the velocity. These results suggest that clathrin coats may not exist as inert, transient structural configurations, and that the current understanding of the role of plasma-membrane-associated clathrin may be incomplete.

Results and Discussion

Both dsRed-clathrin and GFP-clathrin have been previously observed to exist in puncta adjacent to the plasma membrane which occasionally disappear, presumably via endocytosis (10,20,21). Additionally, these studies suggest that labeled clathrin light chain can assemble into functional clathrin-coated pits: labeled clathrin colocalizes with endogenous clathrin and AP2 and is capable of functioning in assays for transferrin uptake (10,20,21). In experiments previously performed in migrating MDCK cells, a subset of clathrin spots was observed to move laterally along linear trajectories within the evanescent field (20). The population of clathrin puncta moving along linear trajectories had not previously been detailed by other studies analyzing the dynamics of clathrin-mediated endocytosis in living cells (10,21).

To determine if lateral spot motility is a phenomenon common to non-migrating cells, MDCK, CHO, Cos-7 and HeLa cells were evaluated by TIR-FM subsequent to transfection with dsRed-clathrin. Laterally motile spots were observed in non-migrating MDCK cells (Video 1, available in the Video Gallery at www.traffic.dk.) and in each of the other cell lines evaluated: CHO (Figure 1), Cos-7 (data not shown) and HeLa (data not shown). In CHO cells $\sim 2\%$ of spots demonstrated linear lateral motion per minute (84 out of 4535 spots from 10 cells).

In some cases multiple clathrin spots were observed to travel along the same trajectory (Video 1). The average length of the trajectories of 21 laterally motile clathrin spots sampled from four MDCK cells was $2.30 \pm 0.21\,\mu m$ and the average rate of motion was $0.81 \pm 0.06\,\mu m/s$. These values are similar to those previously observed for rates of vesicle movement along the microtubules in the cytosol (12) and along the microtubules adjacent to the plasma membrane (22). This movement was not expected in light of models for the behavior of clathrin adjacent to the cell surface that suggest that coat components polymerize at the sites of endocytosis and that the clathrin coat is rapidly shed following internalization (2,6,12,19).

Excitation in TIR-FM decreas exponentially with distance from the coverglass. As the depth of penetration of the evanescent field ($\sim 100\,nm$) is on the same scale as the diameter of a clathrin-coated vesicle, internalization of clathrin-coated pits is marked by a rapid decrease in fluorescence (10,20). To determine if the laterally motile population of dsRed-clathrin puncta moves during internalization, 37 spots from a total of seven cells were tracked throughout the duration of motion. Only 8% of the spots analyzed disappeared from the evanescent field while undergoing lateral motion; the large majority of spots (34 out of 37) remained in the plasma-membrane-associated region during and immediately following spot movement.

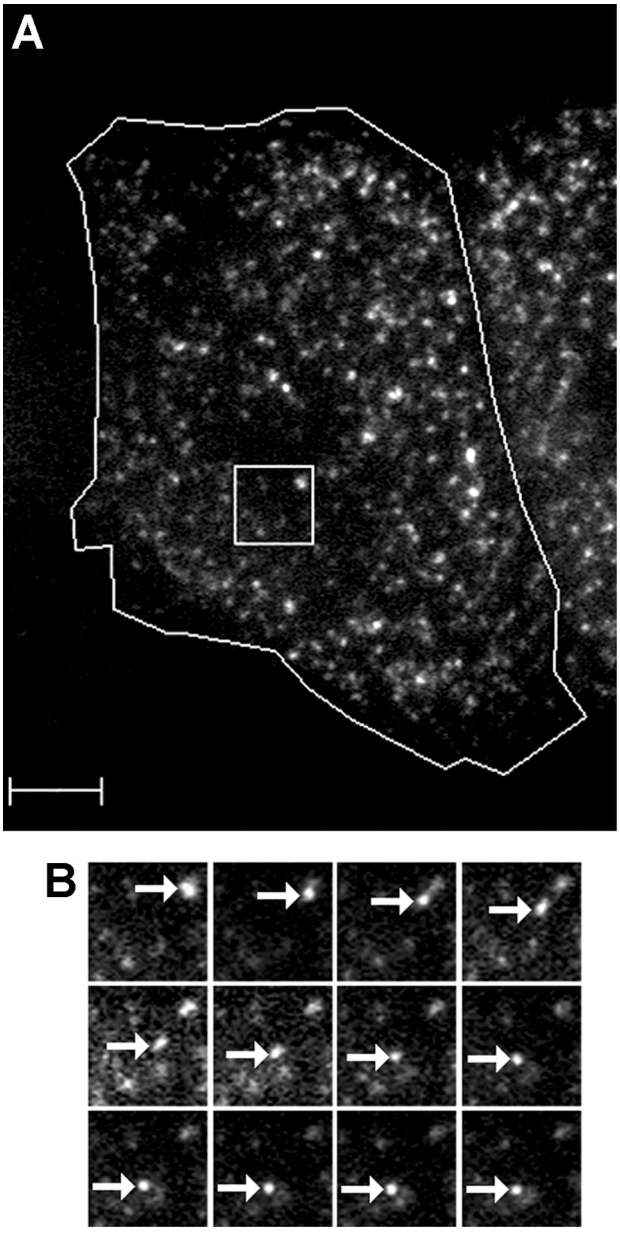

Figure 1: Motility of a dsRed-clathrin spot. A. CHO cell transfected with dsRed-clathrin showing punctate fluorescence in TIR-FM. The scale bar equals 5 μm. B. Linear lateral motion of a dsRed-clathrin spot that stops and is not immediately internalized. Images acquired at 200 ms per frame.

Our analyses of both migrating and stationary cells demonstrate that lateral motion immediately prior to internalization is not a prerequisite for endocytosis. Rather, motile spots remain within the evanescent field throughout, and immediately following, the period of motility.

To test whether there was a relation between movement of clathrin puncta and microtubules, we tested whether: (i) movement of clathrin was coincident with the microtubule cytoskeleton; (ii) expression of a microtubule-associated protein affected the movement of clathrin

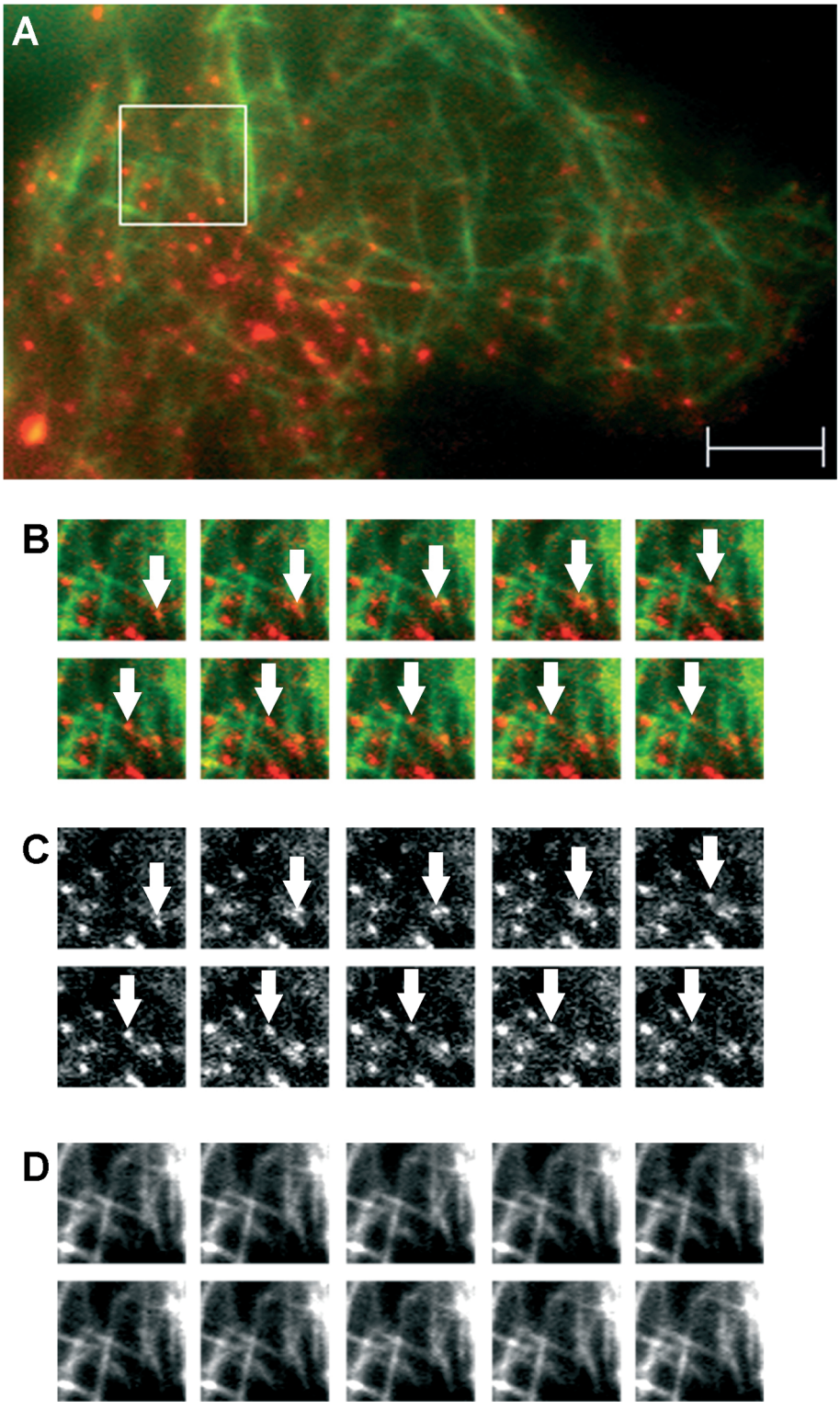

Figure 2: Motility of dsRed-clathrin spots along the MDCK cell microtubule cytoskeleton. A. MDCK cell cotransfected with dsRed-clathrin and tau-EGFP showing the region imaged in B–D. The scale bar equals 5 μm. B–D. Sequential frames from TIR-FM video microscopy of the region outlines in A sampled at 300 ms per frame. B depicts the overlay of the dsRed-clathrin (C) and tau-EGFP (D) images. The arrow depicts the motile dsRed-clathrin spot.

puncta; (iii) depolymerization of the microtubule cytoskeleton affected movement of clathrin. To evaluate whether the lateral movement of clathrin puncta was coincident with microtubules, cells were cotransfected with dsRed-clathrin and markers for the microtubule cytoskeleton, either tau-EGFP or tubulin-EGFP.

In MDCK cells, dsRed-clathrin spots were observed to move along tau-EGFP-labeled microtubules when both fluorophores were imaged simultaneously (Figure 2 and Video 2, Videos available in the Video Gallery at www.traffic.dk.). Similar studies were performed in CHO cells, a cell line derived from both a different species (hamster as opposed to dog) and tissue (ovary as opposed to kidney). Lateral motility of dsRed-clathrin spots along both tubulin-EGFP (Figure 3B) and tau-EGFP (data not shown) stned microtubules was observed. Therefore, the coincidence of motile dsRed-clathrin spots along microtubules is not a function of the particular tag used to identify the microtubule cytoskeleton (tau-EGFP or tubulin-EGFP). These results (Figures 2 and 3) demonstrate that a clathrin-labeled compartment is capable of motility along microtubules, a finding with implications potentially relevant to the studies of both the endocytic and the biosynthetic pathways.

The potential involvement of microtubules in clathrin movement was further evaluated by comparison of spot motility following coexpression of the microtubule binding protein tau, or of tubulin. The run length (Figure 4A) and velocity (Figure 4B) of laterally motile spots was quantified in MDCK cells transfected with dsRed-clathrin alone, or cotransfected with either tau-EGFP or tubulin-EGFP. Although the run length of clathrin puncta was reduced ~40% by tau transfection, this manipulation had no significant effect on spot velocity (Figure 4B). This observation is consistent with the previously reported finding that in cells transfected with tau the motion of post-Golgi vesicles along microtubules shows a decreased run length without any alteration in vesicle velocity (23). Co-transfection with tubulin-EGFP had no significant effect on either run length or velocity, suggesting that the observed effect is specific to the expression of tau and not a result of association of EGFP with microtubules. As these results are similar to those observed in the case of post-Golgi

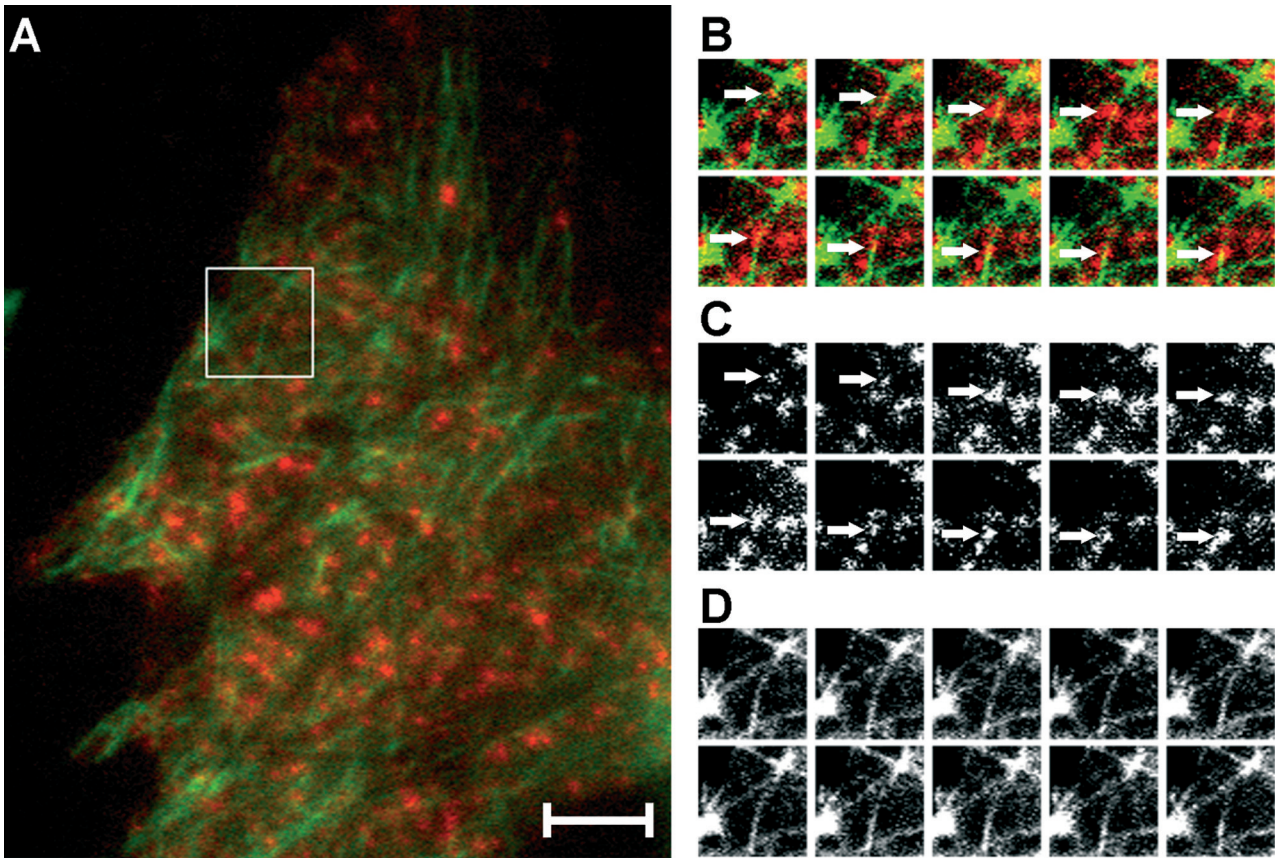

Figure 3: Motility of dsRed-clathrin spots along the CHO cell microtubule cytoskeleton. A. CHO cell cotransfected with dsRed-clathrin and tubulin-EGFP showing the region imaged in B–D. The scale bar equals 5 μm. B–D. Sequential frames from TIR-FM video microscopy of the region outlines in A sampled at 300 ms per frame. B depicts the overlay of the dsRed-clathrin (C) and tubulin-EGFP (D) images. The arrows depict the motile dsRed-clathrin spot.

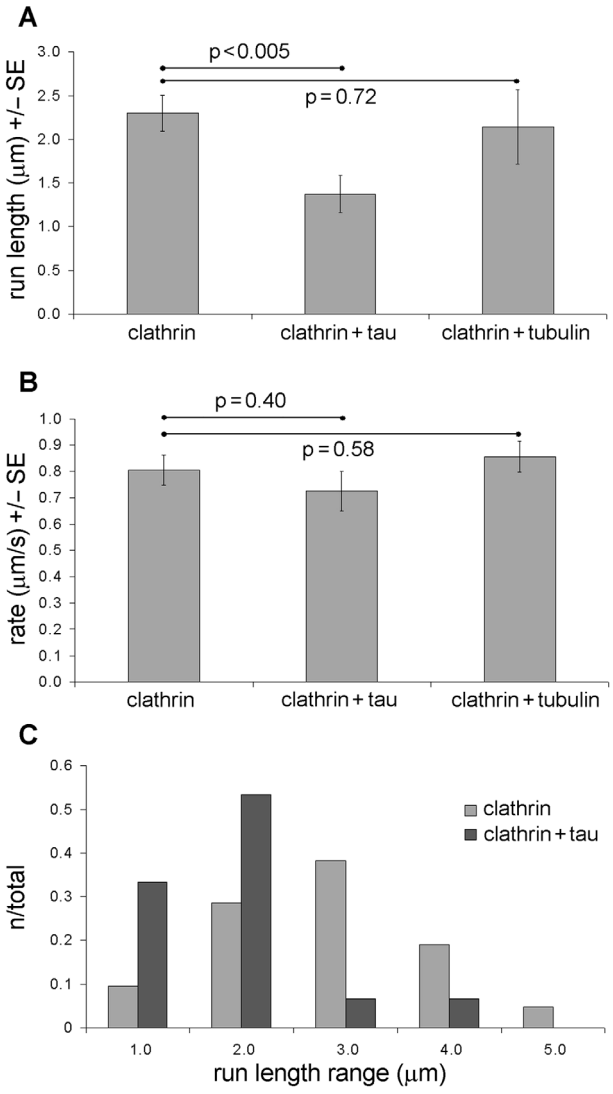

Figure 4: Effect of microtubule labeling on dsRed-clathrin spot motility. A. Bar graph depicting the average run length of motile dsRed-clathrin spots with or without cotransfection with tau-EGFP or tubulin-EGFP. B. Bar graph depicting the average velocity of motile dsRed-clathrin spots with or without cotransfection with tau-EGFP or tubulin-EGFP. C. Run length histogram comp- aring the distance traveled by dsRed-clathrin spots in cells with or without tau-EGFP cotransfection. The number of spots per group are as follows: dsRed-clathrin: 21 spots from 4 cells, dsRed-clathrin + tau-EGFP: 15 spots from 4 cells, and dsRed-clathrin + tubulin-EGFP: 12 spots from 3 cells.

vesicle transport (23), they represent further evidence that this lateral motility is occurring along the microtubule cytoskeleton.

While a significant decrease in motile spot run length was observed following coexpression of the microtubule-associated protein tau, this difference in average distance could have been due to the generation of two distinct populations of motile spots, one moving along trajectories of equivalent length to those in cells not expressing tau-EGFP, and a second group of nearly immobile spots. To differentiate between these possibilities a run length histogram was generated comparing the distributions of spots from cells with and without tau-EGFP coexpression. In cells transfected only with dsRed-clathrin spot run length is distributed in an apparent normal fashion from below 1 μm to between 4 and 5 μm (Figure 4C). However, nearly all of the spots in the cells cotransfected with tau-EGFP moved less than 2 μm. Therefore, the results of the histogram analysis suggest that tau-EGFP coexpression is affecting the motility of all dsRed-clathrin spots, not just a subset.

To test if depolymerization of microtubules would affect the movement of clathrin puncta, cells were treated with nocodazole. CHO cells expressing dsRed-clathrin were imaged before and after nocodazole treatment, and following recovery after nocodazole treatment (Figure 5). In both the TIR-FM (Figure 5A) and epifluorescence images (Figure 5B), nocodazole treatment resulted in a nearly complete loss of tau-EGFP-stained microtubules. The effect of nocodazole was reversible and therefore not lethal to the cells: 24 h after the nocodazole was washed out of the media, the microtubules had repolymerized (Figure 5A,B right panel).

Clathrin spot motility was evaluated before, during and after nocodazole treatment. The number of laterally moving spots was counted in dsRed-clathrin-transfected CHO cells (10 cells per group) with and without nocodazole treatment, and following 24 h of nocodazole withdrawal. Nocodazole treatment was sufficient to nearly completely eliminate the lateral motion of clathrin spots (Figure 5C). In contrast, incubation with cytochalasin D sufficient to disrupt the actin cytoskeleton was not able to arrest clathrin spot motility (data not shown). Following nocodazole removal, however, the lateral movement of clathrin puncta was restored. This implies that the lateral motion of clathrin puncta is directly dependent upon the presence of intact microtubules.

These observations demonstrate that the movement of clathrin puncta is dependent on microtubules: motility is affected by over-expression of a microtubule-associated protein (tau) and it is halted upon depolymerization of microtubules and restored upon repolymerization. This suggests a role for microtubules in the movement of plasma-membrane-associated clathrin puncta. This lateral motion, which is observed in multiple cell lines (MDCK, CHO, Cos-7 and HeLa), does not generally occur during spot internalization. Although it is believed that the plasma membrane and the Golgi apparatus are the main sites of clathrin-coated vesicle formation, the budding of clathrin-positive regions of tubular endosomes has also been reported (24). It remains to be resolved whether these moving spots represent disks of polymerized clathrin on the cytosolic surface of the plasma membrane, clathrin-coated vesicles that have just been endocytosed, but not

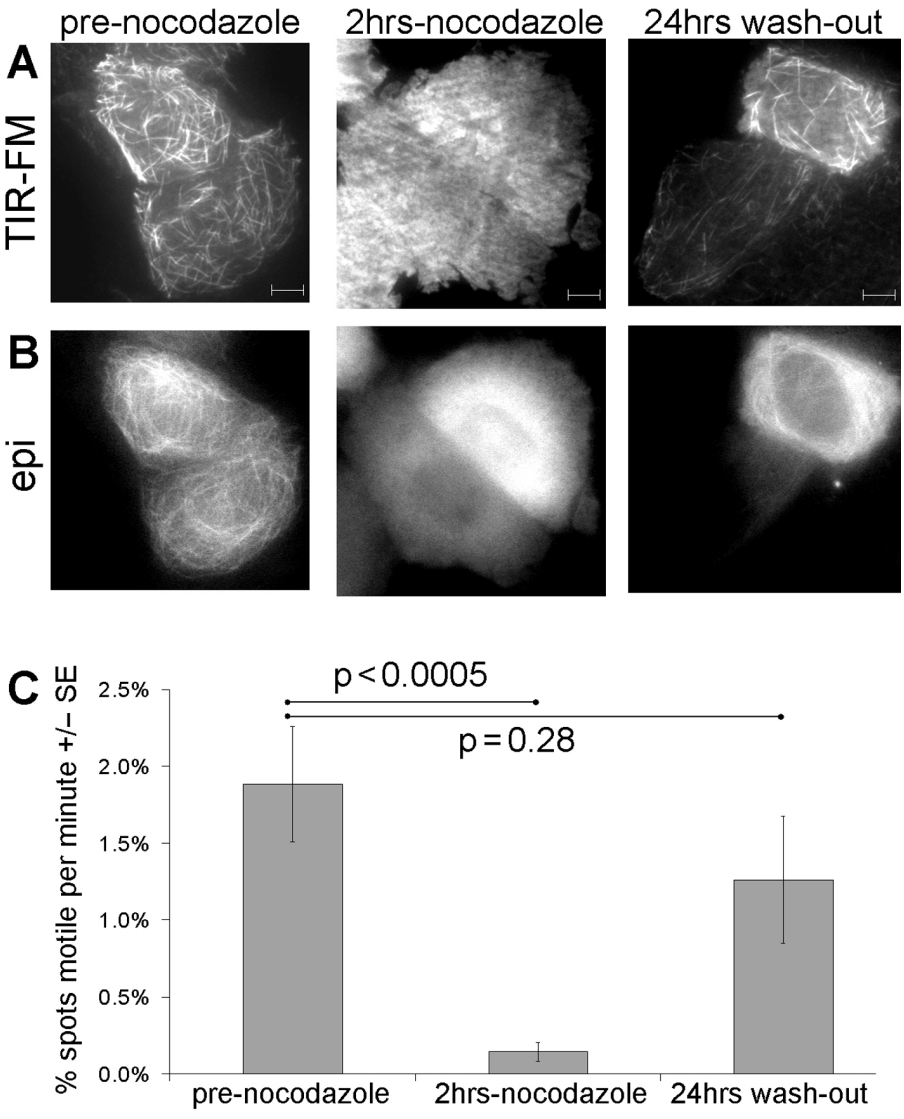

Figure 5: Effects of nocodazole treatment. A and B. TIR-FM (A) and epifluorescence imaging (B) of CHO cell transfected with tau-EGFP before and after nocodazole treatment, and after nocodazole washout. The scale bars equal 5 μm. C. Clathrin spot lateral motility before and after nocodazole treatment, and after nocodazole washout. Motility is depicted as the percentage of motile spots per cell per minute. A total of 10 cells per group were analyzed.

yet separated from the plasma membrane, or yet another organelle. It is possible that the clathrin spots moving along the microtubule cytoskeleton represent structures immediately prior or subsequent to endocytosis, such as clathrin-coated pits or vesicles, respectively, or, alternatively, endosomally derived vesicles moving in a compartment adjacent to the plasma membrane. Thus, these results demonstrate the need for a reevaluation of the functional role of plasma-membrane-associated clathrin (2,6,19).

Materials and Methods

Plasmid constructs

The construct encoding dsRed-clathrin (rat light chain) was a gift of Dr Thomas Kirchhausen of Harvard Medical School (Boston, MA, USA). The construct encoding tau-EGFP was a gift of Dr Peter Mombaerts of the Rockefeller University (New York, NY, USA). Tubulin-EGFP was purchased from Clontech (BD Biosciences Clontech, Palo Alto, CA, USA).

Cell culture

MDCK, CHO, Cos-7 and HeL cells were maintained in DMEM (Mediatech Cellgro, VA, USA) supplemented with 10% FBS in a 37 °C incubator humidified with 5% CO_2. Cells were plated onto sterilized glass coverslips (Fisher Scientific, Atlanta, GA, USA). Cells were plated at approximately 85% confluence 1 day prior to transfection with Lipofectamine 2000 (Invitrogen Corp., Carlsbad, CA, USA) according to the supplier's directions. Cells were imaged 24–48 h post transfection.

Nocodazole treatment

CHO cells were placed in tissue culture media containing 15 μM nocodazole for 2 h in a 37 °C incubator humidified with 5% CO_2. Cells were maintained in nocodazole during imaging.

Cytochalasin D treatment

To depolymerize the actin cytoskeleton, HeLa and MDCK cells were incubated in Cytochalasin D. MDCK cells were incubated in 1 μM Cytochalasin D for up to 1 h and HeLa cells were incubated in 1 or 5 μM Cytochalasin D for up to 1.5 h. Cells were maintained in Cytochalasin D during imaging. These techniques have previously been shown to result in depolymerization of the actin cytoskeleton (22,25,26). Our laboratory has demonstrated via TIR-FM the disruption of actin stress fibers near the plasma membrane following incubation in Cytochalasin D (22).

Image acquisition

TIR-FM was performed as previously described (8,9) utilizing illumination through the microscope objective (Apo 60X NA 1.45, Olympus America Inc., Melville, NY, USA). All studies were performed with an inverted epifluorescence microscope (IX-70, Olympus) placed within a home-built temperature-controlled enclosure set at 32 °C for live cell imaging. The optical configuration used to image dsRed-clathrin included excitation with the 514 nm line of a tunable Argon laser (Omnichrome, model 543-AP A01, Melles Griot, Carlsbad, CA, USA) reflected off a polychroic mirror (442/514pc). All filters, polychroic and dichroic mirrors were obtained from Chroma Technologies Corp. (Brattleboro, VT, USA). Emitted light was then collected through a 560lp filter. Tau-EGFP and tubulin-EGFP were excited by the 488 nm line of the Argon laser reflected off a dichroic mirror (498dclp). EGFP emission was collected through an emission band pass filter (HQ525/50 m). When dsRed-clathrin and tau-EGFP/tubulin-EGFP were imaged simultaneously, both fluorophores were excited with the 488 nm line of the same tunable Argon laser as above reflected off the 498dclp dichroic. Simultaneous image acquisition was performed utilizing an emission splitter (W-view, Hamamatsu Photonics, Hamamatsu City, Japan). The EGFP/dsRed emissions were collected simultaneously through an emission splitter equipped with dichroic mirrors to split the emission (550dclp). The EGFP emission was then collected through an emission band pass filter (HQ525/50 m) and the dsRed through an emission long pass filter (580lp).

The camera utilized to acquire images was a 12-bit cooled CCD (ORCA-ER, Hamamatsu Photonics, Bridgewater, NJ, USA) with a resolution of 1280×1024 pixels [pixel size $= (6.45\ \mu m)^2$]. The camera and a mechanical shutter (Uniblitz, Vincent Associates, Rochester, NY, USA) were controlled by MetaMorph (Universal Imaging, Downingtown, PA, USA). Images were acquired utilizing exposures times between 150 and 300 ms. For video imaging, between 200 and 400 frames were streamed to memory on a PC during acquisition and then saved to hard disk. The depth of the evanescent field was typically $\sim$70–120 nm (8,9). Processing and analysis of video sequences and still frames was done with MetaMorph, Photoshop 5.5 (Adobe Systems Inc., San Jose, CA, USA) and Excel (Microsoft Corp., Redmond, WA, USA). Image noise was reduced through background subtraction and digital brightness and contrast adjustment.

Determination of the motile proportion of spots

All of the spots observed to move in a linear lateral trajectory for 10 dsRed-clathrin transfected CHO cells were counted. The number of motile spots per minute was then divided by the total number of plasma-membrane-associated spots per cell. The total number of spots per cell was estimated by counting the total number of spots from within three circular regions (area = 2776 pixels) and multiplying the average of the three regions by the total area of the cell divided by the area per region.

Dual-color processing

Dual-color image streams were acquired so that the separated channels appear side by side on the camera chip. Regions of the same size were removed from the whole field to yield separated image sequences. The two channels (GFP and dsRed) were aligned by placing brightfield images of the cells being analyzed on top of the stack of TIR images. The brightfield images were then aligned by eye and then the TIR stacks were similarly aligned according to the same spatial adjustments. Following image alignment, correlation coefficients were obtained (via MetaMorph) following pixel shift of the red image planes 1 pixel at a time for 10 pixels in each direction. Each of the four resultant correlation coefficients for each pixel shift step was then averaged. Alignment was verified by the exponential decrease in correlation coefficient following pixel shift.

Online supplemental material

Two TIR-FM videos are included to illustrate the dynamic motion of dsRed-clathrin spots parallel to the plane of the plasma membrane. Video 1 illustrates the motion of several dsRed-clathrin spots along a linear trajectory, and Video 2 demonstrates the motion of a dsRed-clathrin spot along a tau-EGFP-stained microtubule. Both videos are of live, transiently transfected MDCK cells, and Video 2 represents overlays of simultaneously acquired two-channel (red and green) video microscopy.

Acknowledgments

The authors thank Jyoti Jaiswal and Marina Fix for their critical evaluation of this manuscript. This work was supported by NSF BES 0110070 and NSF BES-0119468 to SMS.

References

1. Doxsey SJ, Brodsky FM, Blank GS, Helenius A. Inhibition of endocytosis by anti-clathrin antibodies. Cell 1987;50:453–463.
2. Schmid SL. Clathrin-coated vesicle formation and protein sorting: an integrated process. Annu Rev Biochem 1997;66:511–548.

3. ter Haar E, Musacchio A, Harrison SC, Kirchhausen T. Atomic structure of clathrin: a beta propeller terminal domain joins an alpha zigzag linker. Cell 1998;95:563–573.
4. Altschuler Y, Barbas SM, Terlecky LJ, Tang K, Hardy S, Mostov KE, Schmid SL. Redundant and distinct functions for dynamin-1 and dynamin-2 isoforms. J Cell Biol 1998;143:1871–1881.
5. Benmerah A, Lamaze C, Begue B, Schmid SL, Dautry-Varsat A, Cerf-Bensussan N. AP-2/Eps15 interaction is required for receptor-mediated endocytosis. J Cell Biol 1998;140:1055–1062.
6. Kirchhausen T. Clathrin adaptors really adapt. Cell 2002;109:413–416.
7. Axelrod D. Cell-substrate contacts illuminated by total internal reflection fluorescence. J Cell Biol 1981;89:141–145.
8. Schmoranzer J, Goulian M, Axelrod D, Simon SM. Imaging constitutive exocytosis with total internal reflection fluorescence microscopy. J Cell Biol 2000;149:23–32.
9. Lampson MA, Schmoranzer J, Zeigerer A, Simon SM, McGraw TE. Insulin-regulated release from the endosomal recycling compartment is regulated by budding of specialized vesicles. Mol Biol Cell 2001;12:3489–3501.
10. Merrifield CJ, Feldman ME, Wan L, Almers W. Imaging actin and dynamin recruitment during invagination of single clathrin-coated pits. Nat Cell Biol 2002;4:691–698.
11. Tsuboi T, Terakawa S, Scalettar BA, Fantus C, Roder J, Jeromin A. Sweeping model of dynamin activity. Visualization of coupling between exocytosis and endocytosis under an evanescent wave microscope with green fluorescent proteins. J Biol Chem 2002;277: 15957–15961.
12. Apodaca G. Endocytic traffic in polarized epithelial cells. role of the actin and microtubule cytoskeleton. Traffic 2001;2:149–159.
13. Merrifield CJ, Moss SE, Ballestrem C, Imhof BA, Giese G, Wunderlich I, Almers W. Endocytic vesicles move at the tips of actin tails in cultured mast cells. Nat Cell Biol 1999;1:72–74.
14. Elkjaer ML, Birn H, Agre P, Christensen EI, Nielsen S. Effects of microtubule disruption on endocytosis, membrane recycling and polarized distribution of Aquaporin-1 and gp330 in proximal tubule cells. Eur J Cell Biol 1995;67:57–72.
15. Hamm-Alvarez SF, Sheetz MP. Microtubule-dependent vesicle transport. modulation of channel and transporter activity in liver and kidney. Physiol Rev 1998;78:1109–1129.
16. Subtil A, Dautry-Varsat A. Microtubule depolymerization inhibits clathrin coated-pit internalization in non-adherent cell lines while interleukin 2 endocytosis is not affected. J Cell Sci 1997;110:2441–2447.
17. Bohm KJ, Vater W, Steinmetzer P, Unger E. Can coated vesicles bind directly to microtubules? Acta Histochem Suppl 1991;41:65–72.
18. Orzech E, Livshits L, Leyt J, Okhrimenko H, Reich V, Cohen S, Weiss A, Melamed-Book N, Lebendiker M, Altschuler Y, Aroeti B. Interactions between adaptor protein-1 of the clathrin coat and microtubules via type 1a microtubule-associated proteins. J Biol Chem 2001;276: 3134–31348.
19. Takei K, Haucke V. Clathrin-mediated endocytosis: membrane factors pull the trigger. Trends Cell Biol 2001;11:385–391.
20. Rappoport JZ, Simon SM. Real-time analysis of clathrin-mediated endocytosis during cell migration. J Cell Sci 2003;116:847–855.
21. Gaidarov I, Santini F, Warren RA, Keen JH. Spatial control of coated-pit dynamics in living cells. Nat Cell Biol 1999;1:1–7.
22. Schmoranzer J, Simon SM. Role of microtubules in the fusion of post-Golgi vesicles to the plasma membrane. Mol Biol Cell 2003;14: 1558–1569.
23. Trinczek B, Ebneth A, Mandelkow EM, Mandelkow E. Tau regulates the attachment/detachment but not the speed of motors in microtubule-dependent transport of single vesicles and organelles. J Cell Sci 1999;112 (Pt 14):2355–2367.
24. Stoorvogel W, Oorschot V, Geuze HJ. A novel class of clathrin-coated vesicles budding from endosomes. J Cell Biol 1996;132:21–33.
25. Bennett EM, Chen CY, Engqvist-Goldstein AE, Drubin DG, Brodsky FM. Clathrin hub expression dissociates the actin-binding protein Hip1R from coated pits and disrupts their alignment with the actin cytoskeleton. Traffic 2001;2:851–858.
26. Bricker JL, Chu S, Kempson SA. Disruption of F-actin stimulates hypertonic activation of the BGT1 transporter in MDCK cells. Am J Physiol Renal Physiol 2003;284:F930–F937.